SPE · AAPG · SEG
CCUS
Carbon Capture, Utilization, and Storage

CCUS: 4436779

Role of Wettability Heterogeneity and CO_2 Mineralization in Basalts

Prince Otabir[1], Aaditya Khanal[1,2*], 1. Russell School of Chemical Engineering, The University of Tulsa, 2. McDougall School of Petroleum Engineering, The University of Tulsa

This paper was prepared for presentation at the Carbon Capture, Utilization, and Storage conference held in The Woodlands, TX, 30 March – 01 April.

Abstract

While CO_2 storage has traditionally focused on sedimentary formations, basaltic rocks have recently gained attention as promising targets because they have high mineral trapping potential, which depends on several factors, including wettability, which controls how fluids distribute and interact within the rock. Experimental and field studies indicate that wettability in subsurface reservoirs is inherently heterogeneous, and this heterogeneity can significantly affect CO_2 migration and trapping. These effects are further complicated in basaltic formations, where rapid geochemical reactions promote mineralization. In this study, a two-dimensional reactive transport model was developed using a robust compositional simulator to investigate the coupled impacts of wettability heterogeneity and mineralization on CO_2 storage performance in basaltic reservoirs. Three heterogeneous wettability scenarios were considered, consisting of 80%/20%, 50%/50%, and 20%/80% of water-wet/CO_2-wet distributions, implemented through distinct relative permeability and capillary pressure curves. Results show that in the absence of mineralization, water-wet dominant reservoirs promote enhanced lateral CO_2 plume spreading, with approximately 15% greater horizontal extent and 15% reduced vertical migration compared to CO_2-wet dominant reservoirs. When mineralization is included, water-wet dominant reservoirs exhibit the highest mineral trapping efficiency, reaching approximately 48% of the injected CO_2, compared to about 41% in CO_2-wet dominant cases. However, this enhanced trapping is accompanied by increased pressure buildup, revealing a trade-off between long-term storage security and injection performance. This research offers practical guidance for CCUS developers and reservoir simulators to design safer and more reliable carbon storage strategies in basaltic formations. It highlights that wettability heterogeneity is a key factor controlling mineral reactions and overall storage performance and should be explicitly considered in large-scale modeling and project design.

Keywords: CO_2 storage; Wettability Heterogeneity; Basalt; Reservoir Simulation

Introduction

Achieving ambitious global CO_2 emissions reduction targets requires the integration of multiple mitigation technologies. In energy-intensive sectors, carbon capture and storage (CCS) has become a central component of these strategies due to its unique capacity to permanently store large volumes of CO_2 [1]. CCS involves capturing CO_2 from major emission sources and injecting it into deep geological formations such as saline aquifers, depleted oil and gas reservoirs, and coal mines [2]. CO_2 is often trapped through structural, residual, dissolution, and mineral trapping mechanisms, with mineral trapping typically occurring over timescales of thousands of years after injection [3]. Although mineral trapping is a relatively slow process, it represents the most secure storage mechanism, as CO_2 is converted into stable carbonate minerals with minimal risk of leakage [4]. In contrast, basalt formations have been recognized as very promising storage candidates due to the abundance of reactive silicate minerals which readily convert CO_2 into stable carbonates with minimal leakage risk [2,5].

Structural and residual trapping mechanisms typically dominate during the early stages of active injection and the post-injection period, and are highly sensitive to multiphase flow properties such as interfacial tension, wettability, mass transfer, and capillary pressure[6]. Among these properties, wettability controls the spatial distribution of brine and CO_2 within the reservoir. Wettability not only determines structural and residual trapping capacities [7], but also exerts strong control over multiphase flow properties, including relative permeability, capillary pressure, and saturation of aqueous and nonaqueous phases[8]. Despite its importance, wettability remains a complex and incompletely understood parameter, particularly in reservoir rocks[9]. It is most commonly evaluated through contact angle measurements where the rock is classified into either water-wet, mixed-wet, or CO_2-wet [10].

Previous experimental and numerical studies investigating the influence of wettability on CO_2 storage capacity have shown that water-wet rocks tend to limit steep vertical CO_2 migration within the reservoir while enhancing residual trapping mechanisms [11–13]. However, these numerical investigations commonly assume spatially homogeneous wettability distributions. In basaltic reservoirs, available measurements indicate that wettability can vary substantially with storage conditions and basalt type, including a transition from strongly water-wet at shallow conditions to more intermediate-wet behavior at greater depths [14]. Such depth-dependent evolution implies that natural basalt formations are unlikely to exhibit a single uniform wetting state; instead, different reservoir intervals may simultaneously display distinct wettability characteristics, creating spatial heterogeneity in initial wettability states. In addition, basalt wettability is also sensitive to surface alteration and chemical conditioning (e.g., organic aging or surfactant exposure), which can further modify local wetting states and amplify small-scale variability within the rock matrix [15].

These observations motivate the current study. While wettability heterogeneity has extensively investigated in carbonate formations, a significant knowledge gap remains for basalt formations, where mineral trapping through CO_2 mineralization represents a dominant long-term storage mechanism due to the high reactivity of basaltic minerals with CO_2-rich fluids [4]. The interaction between spatially variable wettability and geochemical mineralization processes therefore remains poorly understood in basalt formations. This gap in literature motivates the present study, which systematically investigates the coupled effects of wettability heterogeneity and mineralization on CO_2 storage capacity in basalt reservoirs.

Methodology

In this study, we use the CMG-GEM (version 2025.10) reservoir simulator to model CO_2 mineralization driven by geochemical reactions in a basaltic reservoir under heterogeneous wettability conditions. The simulator employs the Peng–Robinson equation of state (EOS) to describe the thermodynamic behavior of the CO_2–brine system, enabling the coupled simulation of multiphase flow, mass transport, and geochemical reactions within the reservoir [16].

The 2D reservoir model comprised of 12,000 grid blocks (200 x 1 x 60), spanning a length of 1000 m and height of 100 m, shown in **Figure 1** [17]. The top of the reservoir is located at a depth of 1200 m, with an initial pressure of 11,800 kPa specified at the reservoir top. No-flow boundary conditions are applied along all model boundaries. A centrally located vertical injection well is completed with perforations in grid blocks (200:1:55–57). A total of 1.706×10^6 kg (~1706 metric tons) of CO_2 injected at a rate of 250 m^3/day under standard conditions over a 10-year injection period. The corresponding supercritical CO_2 density at reservoir conditions was ~651 kg/m^3. The simulation is continued for a total duration of 100 years to evaluate long-term trapping behavior. Although this injection rate may appear low compared to field-scale operations, it is consistent with injection rates used in scaled 3D simulation studies (Bump et al [18]). Isothermal conditions are assumed throughout the simulations, with a constant reservoir temperature of 50 ℃. A homogeneous absolute permeability of 1 mD is assigned to the reservoir, with a vertical-to-horizontal permeability ratio (k_v/k_h) of 0.1 and a porosity of 0.18.

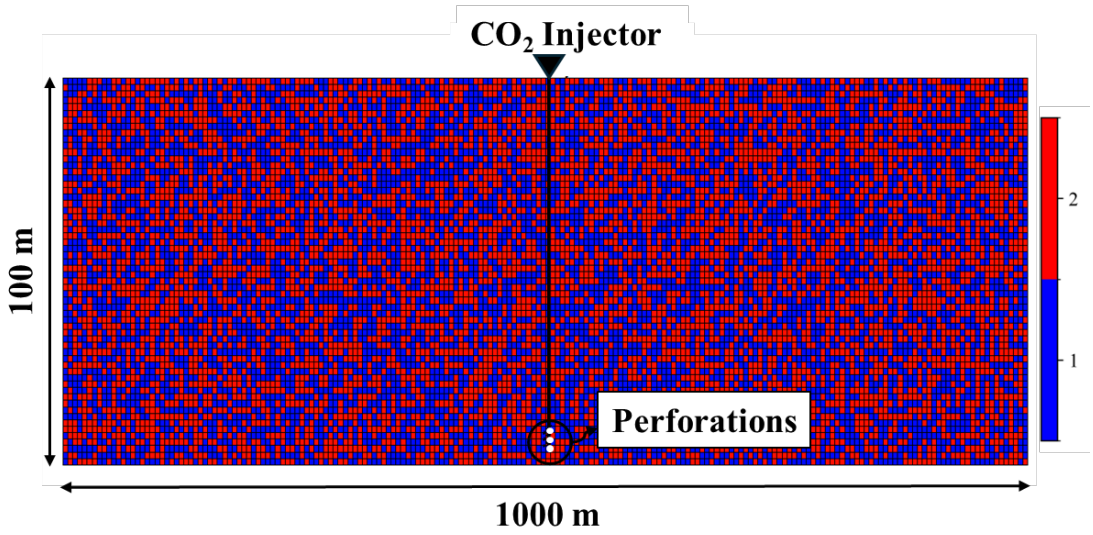

Figure 1–2D reservoir model used in the study. The color map illustrates the spatial distribution of wettability-based rock types, where values of 1 and 2 represent water-wet and CO_2-wet relative permeability and capillary pressure sets, respectively. The distribution shown corresponds to the 50% water-wet and 50% CO_2-wet (WW50-CW50) heterogeneous wettability case.

It is well established that reservoir wettability can vary spatially and that wettability exerts a strong control on capillary pressure, relative permeability, and the resulting residual gas and water saturations [13,19,20]. To represent heterogeneous wetting conditions, two distinct sets of relative permeability and capillary pressure curves were employed in this study, corresponding to water-wet and CO_2-wet conditions. The relative permeability curves were adopted from Al-Khdheeawi et al. [21] and are shown in **Figure 2**. Relative permeability hysteresis was modeled using the Carlson hysteresis model. Capillary pressure curves were described using the Brooks–Corey model (**Eq. 1**), with capillary entry pressure (P_{ce}) values taken from Park et al. [22] i.e., 8.33 kPa for the water-wet case and 1.45 kPa for the CO_2-wet case.

$$P_c = P_{ce} \times \left(\frac{S_w - S_{wi}}{1 - S_{wi}}\right)^{-\frac{1}{\lambda}} \quad (1)$$

S_w is the water saturation, S_{wi} is the initial water saturation, and λ is the pore saturation index [23].

Following experimental observations and previous numerical studies indicating that wettability heterogeneity is often represented using stochastic distributions [13,24,25], a similar approach was adopted in this study. Three wettability distribution scenarios were considered: (i) 80% water-wet and 20% CO_2-

wet (WW80-CW20), (ii) 50% water-wet and 50% CO_2-wet (WW50-CW50), and (iii) 20% water-wet and 80% CO_2-wet (WW20-CW80) using two wettability defined rock types for water-wet and CO_2-wet rocks, respectively. **Figure 1** shows the 50% water-wet and 50% CO_2-wet case. These cases enable a systematic assessment of the impact of wettability heterogeneity on CO_2 plume migration and trapping behavior.

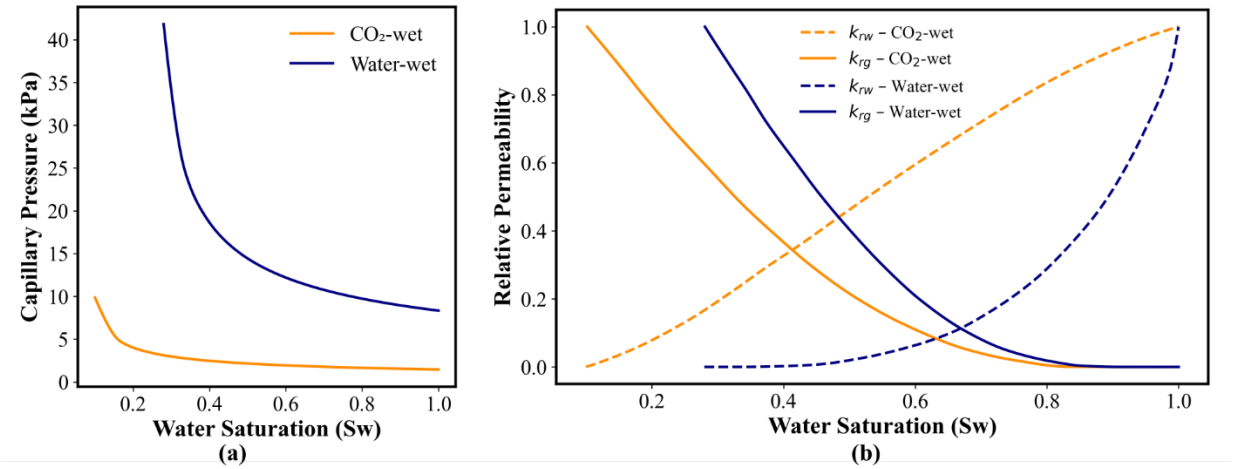

Figure 2–(a) Capillary Pressure Curves and (b) Relative Permeability Curves for CO_2-wet and water-wet conditions.

The primary basaltic minerals considered in the geochemical model include forsterite, wollastonite, enstatite, and anorthite [26]. The initial volume fractions assigned to these minerals are 21.42% for enstatite, 20.97% for forsterite, 35.87% for anorthite, and 1.73% for wollastonite, which are representative of crystalline basalt mineral assemblages. The secondary minerals allowed to precipitate during the simulations include magnesite and calcite. The corresponding mineral dissolution and precipitation reactions considered in the model are listed below:

$$Forsterite(Mg_2SiO_4) + 4H^+ \leftrightarrow 2H_2O + 2Mg^{2+} + SiO_2(aq) \quad (a)$$

$$Wollastonite(CaSiO_3) + 2H^+ \leftrightarrow H_2O + Ca^{2+} + SiO_2(aq) \quad (b)$$

$$Enstatite(MgSiO_3) + 2H^+ \leftrightarrow H_2O + Mg^{2+} + SiO_2(aq) \quad (c)$$

$$Anorthite\ (CaAl_2Si_2O_8) + 8H^+ \leftrightarrow 4H_2O + Ca^{2+} + 2Al^{3+} + 2SiO_2(aq) \quad (d)$$

$$Magnesite(MgCO_3) + H^+ \leftrightarrow Mg^{2+} + HCO_3^- \quad (e)$$

$$Calcite(CaCO_3) + H^+ \leftrightarrow Ca^{2+} + HCO_3^- \quad (f)$$

These mineral reactions proceed at relatively slow rates and are therefore described using kinetic rate laws [27]:

$$r_\alpha = \widehat{A_\alpha} \cdot k_\alpha \left(1 - \frac{Q_\alpha}{K_{eq,\alpha}}\right), \alpha = 1,2,\dots,R_{mn} \quad (2)$$

where r_α is the reaction rate of mineral α, k_α is the rate coefficient, $\widehat{A_\alpha}$ is the effective reactive surface area, Q_α is the ion activity product, and $K_{eq,\alpha}$ represents the corresponding chemical equilibrium constant. **Figure 3** shows the mineral change ($\Delta gmole$) for the specific minerals considered in this study with forsterite undergoing significant dissolution to precipitate magnesite while calcite precipitation is dependent on wollastonite dissolution.

A brine salinity of 10,000 ppm NaCl was specified [28]. The initial aqueous composition includes Ca^{2+}, Al^{3+}, H^{+}, Mg^{2+}, SiO_2, and HCO_3^{-}, with concentrations adapted from Deng et al. [17] and an initial pH of 7 [29].

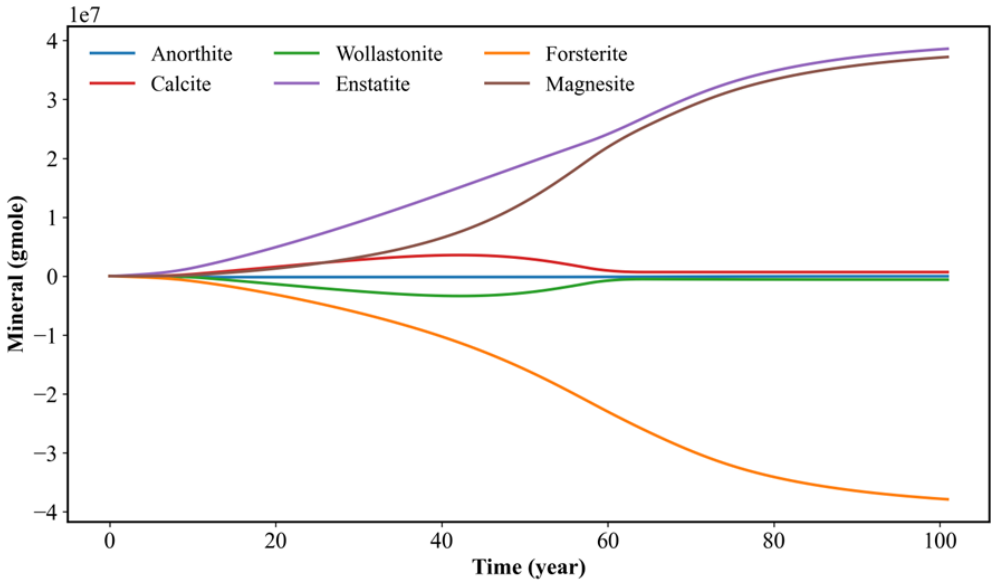

Figure 3–Mineral evolution trends over entire simulation period (100 years).

Results and Discussion

Mineralization was first excluded to investigate the impact of the different heterogeneous conditions on CO_2 migration and plume extents. **Figure 4** illustrates the spatial distribution of CO_2 gas saturation (S_g) at the end of the simulation period (100 years) for the three heterogeneous wettability scenarios. In the water-wet dominant case (WW80-CW20), the CO_2 plume exhibits enhanced lateral spreading, with a horizontal extent of approximately 135 m and a vertical rise of about 43.4 m. As the fraction of CO_2-wet regions increases, a progressive shift in plume geometry is observed. In the WW50-CW50 case, the plume shows a reduced lateral extent and an increased vertical migration height. This trend becomes more pronounced in the CO_2-wet dominant case (WW20-CW80), where the plume is more vertically focused, with a lateral extent 15% lower and vertical extent 15% higher than the water-wet dominant case. These trends are consistent with previous numerical findings by Al-Khdheeawi et al. [30], who reported that higher capillary entry pressures in water-wet systems restrict upward CO_2 migration and promote lateral plume spreading.

Although the plume geometry clearly follows the expected directional trend with changing wettability, the magnitude of change is modest relative to the large, imposed contrast in wettability fraction. This suggests that CO_2 migration responds to wettability distribution in a moderated manner, as spatial variations in wetting state redistribute flow paths and reduce the overall sensitivity of plume development to wettability fraction.

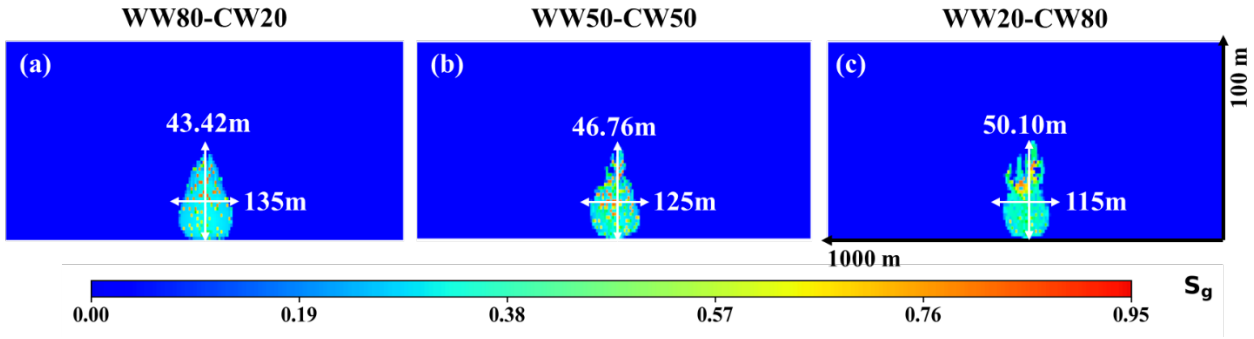

Figure 4–CO_2 plume migration for the three heterogeneous wettability conditions at the end of the simulation period. The CO_2-wet dominant case (WW20-CW80) heterogeneous case exhibited the highest vertical migration.

CO_2 mineralization was now incorporated into the analysis, and the resulting CO_2 trapping contributions are shown in **Figure 5**. The figure presents the partitioning of trapped CO_2 among the three heterogeneous wettability scenarios considered in this study. At the end of the simulation period, mineral trapping and dissolved CO_2 clearly dominate the overall trapping, while residual and mobile CO_2 constitute only minor fractions.

The mobile CO_2 fraction remains small primarily because rapid mineralization consumes a large portion of the free CO_2 available in the reservoir, thereby limiting both mobile and residual contributions to less than ~9% and 5%, respectively for all cases. A clear wettability dependent trend, however, is observed. As CO_2-wet conditions become dominant, the mineral trapping efficiency decreases from ~48% to 41%, highlighting the strong influence of wettability on mineral trapping performance in basalt reservoirs. These observations are consistent with findings reported by Khoramian et al. [31], who reported enhanced mineral dissolution as wetting conditions shifted from CO_2-wet to water-wet. The 7% difference in mineral trapping, however, seems minimal when compared to the large, imposed contrast in reservoir-wide wettability fractions, suggesting that mineralization is influenced by the wettability of the regions contacted by the migrated CO_2 plume rather than by the overall assigned wettability fraction alone. Although a greater proportion of water-wet zones increases the likelihood that the plume encounters water-wet regions, CO_2-wet zones remain present within the flow path, resulting in a mixed-wettability interaction that moderates the overall mineralization response.

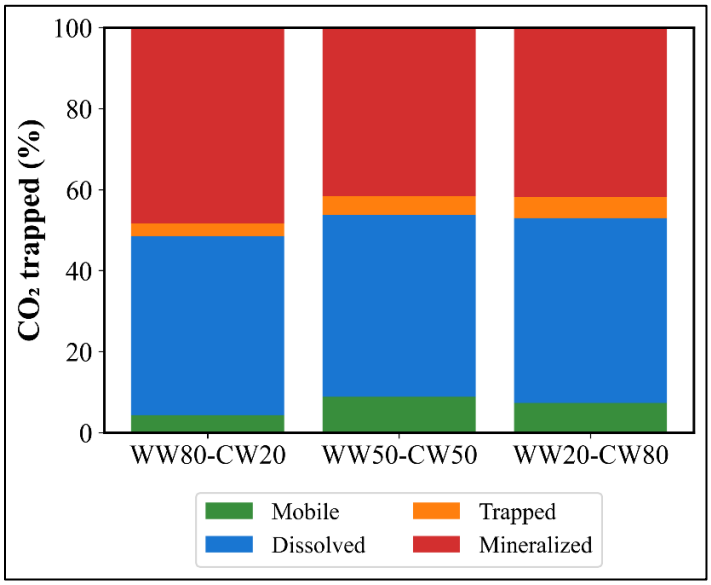

Figure 5–CO_2 trapping contributions across different heterogeneous wettability conditions.

Figure 6 presents the well bottom-hole pressure (BHP) for the three heterogeneous wettability scenarios at the start of injection (1 year) and at the end of the injection period (10 years), highlighting the influence of wettability heterogeneity on pressure buildup during CO_2 injection. At 1 year, the WW80–CW20 case exhibits the highest BHP of ~14,650 kPa, followed by the WW50–CW50 case at ~14,500 kPa, while the WW20–CW80 case shows the lowest BHP of ~14,450 kPa. This early-time response reflects

increased flow resistance in the water-wet dominant reservoir associated with enhanced mineral trapping near the injection region.

As injection progresses, these differences persist and become more pronounced. At the end of the 10-year injection period, the WW80–CW20 case maintains the highest BHP (~15,200 kPa), whereas the WW50–CW50 and WW20–CW80 cases exhibit progressively lower pressures of ~15,150 kPa and 15,100 kPa, respectively. The higher pressure buildup observed in the WW80–CW20 case is attributed to the intensified geochemical reaction in the water-wet fractions of the reservoir, where greater CO_2-brine contact promotes the dissolution of primary minerals and subsequent precipitation of carbonates. This mineral precipitation clogs pore spaces near the injection well, reducing permeability and increasing flow resistance. As a result, pressure near the well increases.

These results reveal a critical coupling between wettability heterogeneity, reactive transport, and injectivity evolution. While water-wet dominant sections of a reservoir may favor enhanced mineral trapping, they also experience greater pressure buildup during injection, potentially leading to injectivity limitations. This highlights a fundamental tradeoff between maximizing long-term storage security through mineralization and maintaining operational injectivity.

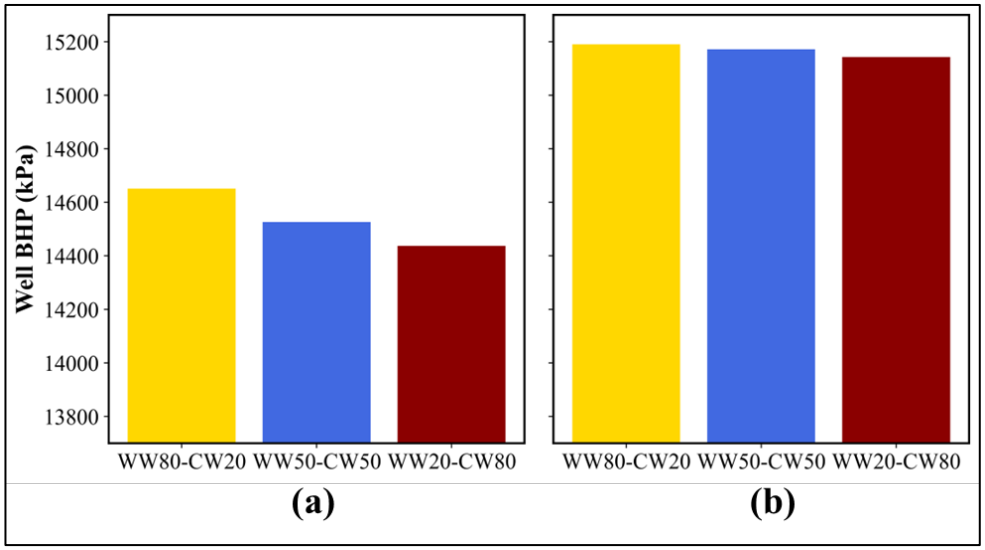

Figure 6–Well BHP at (a) 1 year and (b) 10 years for the different wettability heterogeneity conditions.

For CCUS developers, this pressure-based trade-off underscores the need to balance allowable injection pressures with long-term storage security when designing injection strategies and selecting storage sites. For reservoir simulators, the findings emphasize that wettability heterogeneity and its coupling with geochemical reactions must be explicitly represented to reliably predict pressure evolution, injectivity constraints, and long-term trapping performance.

Conclusions

This study examined the coupled effects of wettability heterogeneity and mineralization on CO_2 plume migration, trapping mechanisms, and injectivity in basalts. The key findings are summarized as follows:

- In the absence of mineralization, water-wet dominant reservoirs (WW80-CW20) were characterized with 15% greater lateral plume spread and 15% reduced vertical migration compared to CO_2-wet dominant reservoirs (WW20-CW80).

- When geochemical reactions were included, water-wet dominant reservoirs exhibited the lowest fraction of mobile CO_2 and the highest mineral trapping efficiency, reaching ~48% of the total trapped CO_2, compared to ~41% in the CO_2-wet dominant reservoir.
- CO_2-wet–dominant reservoirs maintained lower pressure buildup but at the expense of reduced mineral trapping, highlighting competing objectives between injection efficiency and long-term storage permanence.

These findings demonstrate that wettability heterogeneity and mineralization are strongly coupled phenomena that jointly govern CO_2 plume evolution, trapping efficiency, pressure evolution, and injection performance in basaltic reservoirs.

Acknowledgments

We are grateful to the anonymous reviewers for their valuable edits and suggestions, which have significantly enhanced our manuscript. This material is based upon work partly supported by the National Science Foundation Award under CBET2245484. Any opinions, findings, and conclusions or recommendations expressed in this material are those of the author(s) and do not necessarily reflect the views of the National Science Foundation.

References

[1] M.I. Khan, A. Khanal, Machine Learning Assisted Prediction of Porosity and Related Properties Using Digital Rock Images, ACS Omega (2024). https://doi.org/10.1021/acsomega.3c10131.

[2] A. Raza, G. Glatz, R. Gholami, M. Mahmoud, S. Alafnan, Carbon mineralization and geological storage of CO2 in basalt: Mechanisms and technical challenges, Earth-Science Rev. 229 (2022) 104036. https://doi.org/10.1016/j.earscirev.2022.104036.

[3] G.P.D.P.D. De Silva, P.G.G. Ranjith, M.S.A.S.A. Perera, Geochemical aspects of CO2 sequestration in deep saline aquifers: A review, Fuel 155 (2015) 128–143.

[4] P.N.Y.M. Otabir, A. Khanal, F. Nath, Geochemical Impacts of CO2 Mineralization in Carbonate and Basalt Formations: A Critical Review on Challenges and Future Outlook, Energy & Fuels (2025). https://doi.org/10.1021/acs.energyfuels.4c04424.

[5] S.M. Rahaman, A.M. Islam, M.M. Alam, M. Anzuman, Data driven prediction of reservoir rock wettability in shale using deep learning and gene expression programming for CCUS, (2026).

[6] D.J. DePaolo, D.R. Cole, Geochemistry of Geologic Carbon Sequestration: An Overview, Rev. Mineral. Geochemistry 77 (2013) 1–14. https://doi.org/10.2138/rmg.2013.77.1.

[7] N.R. Morrow, Capillary Pressure Correlations For Uniformly Wetted Porous Media, J. Can. Pet. Technol. 15 (1976). https://doi.org/10.2118/76-04-05.

[8] C.H. Pentland, R. El-Maghraby, S. Iglauer, M.J. Blunt, Measurements of the capillary trapping of super-critical carbon dioxide in Berea sandstone, Geophys. Res. Lett. 38 (2011) n/a-n/a. https://doi.org/10.1029/2011GL046683.

[9] J. Zhang, Z. Zhao, Z. Xu, X. Zhang, L. Zhang, Surface wettability of sandstone and shale: Implication for CO2 storage, Int. J. Greenh. Gas Control 126 (2023) 103917. https://doi.org/10.1016/j.ijggc.2023.103917.

[10] X. Wang, S. Li, B. Tong, L. Jiang, P. Lv, Y. Zhang, Y. Liu, Y. Song, Multiscale wettability characterization under CO2 geological storage conditions: A review, Renew. Sustain. Energy Rev. 189 (2024) 113956. https://doi.org/10.1016/j.rser.2023.113956.

[11] S. Iglauer, C.H. Pentland, A. Busch, CO2 wettability of seal and reservoir rocks and the implications for carbon geo-sequestration, Water Resour. Res. 51 (2015) 729–774. https://doi.org/10.1002/2014WR015553.

[12] T. Rahman, M. Lebedev, A. Barifcani, S. Iglauer, Residual trapping of supercritical CO2 in oil-wet sandstone, J. Colloid Interface Sci. 469 (2016) 63–68. https://doi.org/10.1016/j.jcis.2016.02.020.

[13] E.A. Al-Khdheeawi, S. Vialle, A. Barifcani, M. Sarmadivaleh, S. Iglauer, Effect of wettability heterogeneity and reservoir temperature on CO2 storage efficiency in deep saline aquifers, Int. J. Greenh. Gas Control 68 (2018) 216–229. https://doi.org/10.1016/j.ijggc.2017.11.016.

[14] S. Iglauer, A.Z. Al-Yaseri, D. Wolff-Boenisch, Basalt-CO2-brine wettability at storage conditions in basaltic formations, Int. J. Greenh. Gas Control 102 (2020) 2013–2015. https://doi.org/10.1016/j.ijggc.2020.103148.

[15] M. Ali, N. Yekeen, A. Alanazi, A. Keshavarz, S. Iglauer, T. Finkbeiner, H. Hoteit, Saudi Arabian basalt/CO2/brine wettability: Implications for CO2 geo-storage, J. Energy Storage 62 (2023) 106921. https://doi.org/10.1016/j.est.2023.106921.

[16] D.Y. Peng, D.B. Robinson, A New Two-Constant Equation of State, Ind. Eng. Chem. Fundam. 15 (1976) 59–64. https://doi.org/10.1021/i160057a011.

[17] H. Deng, C. Yu, Q. Jiang, C. Gu, Y. Luo, Multi-parameter effects on CO2 mineralization in Basalt: A numerical-sensitivity analysis of CO2 storage in Basalt from Sichuan Basin, southwestern China, Energy 335 (2025) 137803. https://doi.org/10.1016/j.energy.2025.137803.

[18] A.P. Bump, S. Bakhshian, H. Ni, S.D. Hovorka, M.I. Olariu, D. Dunlap, S.A. Hosseini, T.A. Meckel, Composite confining systems: Rethinking geologic seals for permanent CO2 sequestration, Int. J. Greenh. Gas Control 126 (2023) 103908. https://doi.org/10.1016/j.ijggc.2023.103908.

[19] A.S. Al-Menhali, S. Krevor, Capillary Trapping of CO2 in Oil Reservoirs: Observations in a Mixed-Wet Carbonate Rock, Environ. Sci. Technol. 50 (2016) 2727–2734. https://doi.org/10.1021/acs.est.5b05925.

[20] F.G. McCaffery, D.W. Bennion, The Effect Of Wettability On Two-Phase Relative Permeabilities, J. Can. Pet. Technol. 13 (1974). https://doi.org/10.2118/74-04-04.

[21] E.A. Al-Khdheeawi, S. Vialle, A. Barifcani, M. Sarmadivaleh, S. Iglauer, Influence of injection well configuration and rock wettability on CO 2 plume behaviour and CO 2 trapping capacity in heterogeneous reservoirs, J. Nat. Gas Sci. Eng. 43 (2017) 190–206. https://doi.org/10.1016/j.jngse.2017.03.016.

[22] S.S. Park, J. Park, T.H. Kim, K.S. Lee, Influence of heterogeneous capillary pressure on CO2 sequestration in different wetting conditions, Proc. Int. Offshore Polar Eng. Conf. 2015-Janua (2015) 1100–1107.

[23] S.C.M. Krevor, R. Pini, L. Zuo, S.M. Benson, Relative permeability and trapping of CO 2 and water in sandstone rocks at reservoir conditions, Water Resour. Res. 48 (2012) 1–16. https://doi.org/10.1029/2011WR010859.

[24] A. Graue, E. Aspenes, T. Bognø, R.. Moe, J. Ramsdal, Alteration of wettability and wettability heterogeneity, J. Pet. Sci. Eng. 33 (2002) 3–17. https://doi.org/10.1016/S0920-4105(01)00171-1.

[25] E. Aspenes, A. Graue, J. Ramsdal, In situ wettability distribution and wetting stability in outcrop chalk aged in crude oil, J. Pet. Sci. Eng. 39 (2003) 337–350. https://doi.org/10.1016/S0920-4105(03)00073-1.

[26] Q. Al Maqbali, S. Hussain, G. Mask, W. Xingru, Numerical Simulation of In-Situ CO2 Mineralization in Mafic Basaltic Formations in Southwest Oklahoma, in: Soc. Pet. Eng. - SPE Oklahoma City Oil Gas Symp. 2023, OKOG 2023, 2023. https://doi.org/10.2118/213084-MS.

[27] Craig M. Bethke, Geochemical Reaction Modeling: Concepts and Applications, Oxford University Press, 1996.

[28] B.P. McGrail, H.T. Schaef, F.A. Spane, J.A. Horner, A.T. Owen, J.B. Cliff, O. Qafoku, C.J. Thompson, E.C. Sullivan, Wallula Basalt Pilot Demonstration Project: Post-injection Results and Conclusions, in: Energy Procedia, Elsevier B.V., 2017: pp. 5783–5790. https://doi.org/10.1016/j.egypro.2017.03.1716.

[29] D.M. Sturmer, R.N. Tempel, M. Reza, Geological carbon sequestration : Modeling mafic rock carbonation using point-source flue gases, Int. J. Greenh. Gas Control 99 (2020) 103106. https://doi.org/10.1016/j.ijggc.2020.103106.

[30] E.A. Al-Khdheeawi, S. Vialle, A. Barifcani, M. Sarmadivaleh, S. Iglauer, Impact of reservoir wettability and heterogeneity on CO2-plume migration and trapping capacity, Int. J. Greenh. Gas Control 58 (2017) 142–158. https://doi.org/10.1016/j.ijggc.2017.01.012.

[31] R. Khoramian, M. Nurmyrza, W. Lee, Influence of Oil-Wet Wettability and Nanoparticle Treatments on Carbonate Rock Dissolution and CO2 Leakage Risk in Saline Aquifers, Energy & Fuels (2025). https://doi.org/10.1021/acs.energyfuels.5c03710.